Novel syntactic foams made of ceramic hollow micro-spheres and starch: theory, structure and properties

Md Mainul Islam and Ho Sung Kim[1]

Discipline of Mechanical Engineering

School of Engineering

Faculty of Engineering and Built Environment

The University of Newcastle

Callaghan, NSW 2308

Australia

Phone +61 2 4921 6211 Fax +61 2 4921 6946

Email: ho-sung.kim@newcastle.edu.au

Abstract

Novel syntactic foams for potential building material applications were developed using starch as binder and ceramic hollow micro-spheres available as waste from coal-fire power stations. Foams of four different micro-sphere size groups were manufactured with either pre- or post-mould gelatinization process. They were of ternary system including voids with a foam density range of approximately 0.33 - 0.44 g/cc. Compressive failure behaviour and mechanical properties of the manufactured foams were evaluated. Not much difference in failure behaviour or in mechanical properties between the two different processes (pre- and post-mould gels) was found for a given binder content. Compressive failure of all syntactic foams was of shear on plane inclined 45° to compressive loading direction. Failure surfaces of most syntactic foams were characterised by debonded micro-spheres. Compressive strength and modulus of syntactic foams were found to be dependant mainly on binder content but mostly independent of micro-sphere size. Some conditions of relativity arising from properties of constituents leading to the rule of mixtures relationships for compressive strength and to understanding of compressive/transitional failure behaviour were developed. The developed relationships based on the rule of mixtures were partially verified. Some formation of starch webs on failure surfaces was discussed.

[1] Corresponding author

Keywords: Syntactic Foams; Starch; Composites; Debonding; Compressive properties

1. Introduction

Syntactic foams are particulate composites made of pre-formed hollow micro-spheres and binder. They can be used in various structural components. When they are used as core materials for sandwich composites, they contribute to increase in specific stiffness. They further contribute to not only reduction in damage and but also prevention of failure of composite systems by inducing their own damage when they are used for protective structural components [1]. Hence, it is important to understand the failure behaviour of syntactic foams. Compressive failure behaviour of syntactic foams has been studied by many researchers. Narkis et al [2, 3] found that failure of syntactic foams with a low concentration of resin is mainly by disintegration under compression. It was reported, however, that a high density syntactic foam containing under compression failed with formation of 45° shear plane [4, 5]. Recently Kim and Oh [6], and Gupta et al [7] have also reported that failure mode of a syntactic foam with relatively high concentration of resin under uniform compression was by shear on inclined planes. Gupta et al [7, 8] highlighted that the shear failure mechanism is affected by specimen aspect ratio. Kim and Plubrai [1] studied low density (0.11 - 0.15 g/cc) glass/epoxy syntactic foams and found that compressive failure was of 'layered crushing'. Factors affecting the compressive failure behaviour, thus, may include various properties of constituents. Understanding of general mechanical behaviour, however, in relation to affecting factors has not been comprehensive.

A wide range of syntactic foams can be made by selecting different materials and consolidating techniques for binder and hollow micro-spheres. The consolidating techniques include coating micro-spheres [2], rotational moulding [9], extrusion [10, 11] and ones that use inorganic binder solution and firing [12], dry resin powder [3, 13-15] for sintering, compaction [6, 16 liquid resin as binder [17] for in situ reaction injection moulding, and buoyancy [1]. In this paper, new syntactic foams consisting of ceramic hollow micro-spheres and starch have been developed using one of aforementioned manufacturing methods (buoyancy) [1, 18, 19] for potential applications in building materials such as interior sandwich panels etc where the material cost is a driving factor. Starch as binder for syntactic foams has not been employed in the past despite the fact that starch has some advantages over other binders such as epoxies, phenolics, etc

in some applications. It is readily available, environmentally friendly, and an inexpensive renewable polymeric binder although it is dimensionally unstable during manufacturing. The ceramic hollow micro-spheres used for this paper is also inexpensive and available as waste product from coal-fire power stations.

Also in this paper, mechanical behaviour of the novel foams under compression is studied for four different size groups of hollow micro-spheres and various starch contents within a newly proposed theoretical framework.

2. Transitions of mechanical behaviour and rules of mixtures of syntactic foams in ternary system

It is important to identify transitions of mechanical behaviour for understanding failure of syntactic foams and for development of relationships based on the rule of mixtures for various properties.

Figure 1 is the ternary system diagram for micro-spheres, binder and voids (between micro-spheres). The location of point *A* on the voids-micro-spheres axis depends on the way of packing micro-spheres without binder [13] and size distribution of micro-spheres. Point *B* on the micro-sphere-binder axis indicates a volume ratio of binder to micro-spheres when the void fraction is zero. When the void volume fraction decreases and simultaneously the binder volume fraction increases, the composition of the volume fractions of three constituents follows the line from *A* to *B*. The slope of line *A*-*B* depends on volume fraction ratio of three constituents. It is in parallel with the voids-binder axis when an amount of decreased void volume is replaced by the same amount of binder volume for a given constant micro-sphere volume fraction; it is higher than that of the voids-binder axis when voids are replaced by binder whose volume is higher than that of voids; or it is otherwise lower.

Compressive mechanical behaviour of syntactic foams is dependant upon properties and volume fractions of constituents, and geometry of micro-spheres such as ratio of micro-sphere diameter to wall thickness. Position *A* is the point at which no structural strength exists. However, as the binder is added, the syntactic foam begins to have a structural strength. Syntactic foams in the range between point *A* and point α still are not structurally useful and thus failure mode is mainly of gross disintegration as addressed in the literature [1, 2]. As binder content increases past point α, however, syntactic foams become useful as structures and

further their mechanical behaviour is affected by various conditions arising from relative properties of constituents and relativity between load carrying capacities of constituents.

The compressive (uni-axial) load carrying capacity of syntactic foam (F_{sy}) is given by

$$F_{sy} = F_{ms} + F_b \quad (1)$$

where F_{ms} is the load carrying capacity of micro-spheres and F_b is the load carrying capacity of binder.

As volume fractions of constituents vary, two cases are possible i.e. $F_{ms} > F_b$ and $F_{ms} < F_b$.

The first case [$F_{ms} > F_b$] takes place when binder content is low so that micro-spheres take up more load than binder up to the point β (in **Figure 1**). However, as the binder content increases, the second case ($F_{ms} < F_b$) occurs in region β-B so that β is a transitional point between the two cases or a point where $F_{ms} = F_b$.

In the first case of [$F_{ms} > F_b$], bonding strength (σ_{bond}) between micro-spheres and binder in relation with shear strength (σ_{ms}^{s}) can be considered. Two different conditions are possible i.e. $\sigma_{ms}^{s} < \sigma_{bond}$ and $\sigma_{ms}^{s} > \sigma_{bond}$ as will be discussed below.

When the condition of [$F_{ms} > F_b$ and $\sigma_{ms}^{s} < \sigma_{bond}$] takes place, A possible failure mode under the condition is of shear as will be shown later. In this case, shear stress of binder ($\sigma_b^{s'}$) does not reach the shear strength of binder (σ_b^{s}) at the time microspheres fail so that $\sigma_b^{s'} < \sigma_b^{s}$. Shear failure surface would consist of shear failed broken micro-spheres and binder areas which are proportional to respective volume fractions (v_{ms} and v_b). Therefore, the rule of mixtures relationship for shear strength (σ_{sy}^{s}) and compressive strength (σ_{sy}^{c}) of syntactic foam can be obtained as:

$$\sigma_{sy}^{s} = \sigma_b^{s'} v_b + \sigma_{ms}^{s} v_{ms} \quad (2)$$

or

$$\sigma_{sy}^{c} = 2\sigma_{b}^{s'} v_b + 2\sigma_{ms}^{s} v_{ms} \quad \text{(for 45° shear plane - see \textbf{Figure 2} and Equation (8))} \qquad (3)$$

where, if shear strains of binder and micro-spheres (γ_b and γ_{ms} respectively) are equal at fracture (iso-strain condition),

$$\sigma_{b}^{s'} = G_b \gamma_{ms}^{'} \qquad (4)$$

where G_b is the shear modulus of binder and $\gamma_{ms}^{'}$ is the shear strain of micro-spheres at fracture.

When the condition of [$F_{ms} > F_b$ and or $\sigma_{ms}^{s} > \sigma_{bond}$] takes place, however, micro-spheres do not fail but debonding between binder and micro-spheres occurs. Once debonding occurred, binder alone is not capable of further resisting to an increasing compressive load, resulting in total failure of syntactic foam. Thus, fracture surfaces of syntactic foams consist of mainly unbroken micro-spheres as will be seen later (**Figure 6**). The compressive strength (σ_{sy}^{c}) of syntactic foams, therefore, is mainly dependant upon bond strength (σ_{bond}) particularly for a low binder content (generally dependant upon σ_{bond} and/or σ_{b}^{s}) but independent of strength of micro-spheres. When shear failure occurs as illustrated in **Figure 2(a)**, shear strength of syntactic foam (σ_{sy}^{s}) depends on debonding area (A_{bond}) which is larger than an ideally straight cut area of binder (A_{ideal}) inclined 45° to compressive loading direction. The A_{ideal} is proportional to volume fraction of binder (v_b). Thus, it is not unreasonable to assume that debonding area is proportional to volume fraction of binder (v_b) to develop a rule of mixtures relationship for syntactic foam shear strength (σ_{sy}^{s}) given by

$$\sigma_{sy}^{s} = C' \sigma_{bond}\ v_b \qquad (5)$$

or

$$\sigma_{sy}^{c} = C\sigma_{bond}\ v_b \tag{6}$$

where *C'* and *C* are proportional constants.

In the second case of [$F_{ms} < F_b$] where volume fraction of binder is relatively high, the relativity between σ_{ms}^{s} and σ_{bond} is no longer of major issue in development of a rule of mixtures relationship for compressive/shear strength of syntactic foam because binder alone is capable of carrying load irrespective of bonding state even after failure of micro-spheres. Thus, relativity between fracture strains of micro-spheres and binder ($\gamma_{ms}^{'}$ and $\gamma_{b}^{'}$ respectively) appears to be appropriate to be considered for imposition of conditions (see below).

When the condition of [$F_{ms} < F_b$, $\gamma_{ms}^{'} < \gamma_{b}^{'}$] takes place, micro-spheres fail first on shear plane (if shear failure occurs) and then binder takes over the loading up to a point at which binder fails (see **Figure 2(b)**). In this case, the more micro-spheres the lower shear strength of syntactic foam for a given void volume fraction (v_v) until $F_{ms} = F_b$ if the iso-strain condition applies. The compressive strength of syntactic foam (σ_{sy}^{c}) therefore becomes

$$\sigma_{sy}^{s} = \sigma_{b}^{s} v_b = \sigma_{b}^{s}(1 - v_{ms} - v_v) \tag{7}$$

or

$$\sigma_{sy}^{c} = \frac{\sigma_{b}^{s} A_{b}^{s} / \sin\theta}{A_{sy}^{c}}$$

$$= 2\sigma_{b}^{s} v_b \ (\text{if } \theta = 45°) \tag{8}$$

where θ is the angle shown in **Figure 2(b)**, A_b^s is the shear area of binder, A_{sy}^s is the shear area of syntactic foam, and A_{sy}^c is the normal compressive area of syntactic foam.

When the condition of [$F_{ms} < F_b$, $\gamma_{ms}^{'} > \gamma_b^{'}$] takes place, binder fails on shear plane first (if shear failure occurs) and immediately is followed by micro-sphere failure because micro-spheres alone are not capable of carrying further load. Therefore, micro-spheres contribute to the compressive strength of syntactic foam (σ_{sy}^c) but at a stress lower than its shear strength (σ_{ms}^s) so that, if the iso-strain condition applies,

$$\sigma_{sy}^c = 2\sigma_b^s v_b + 2\sigma_{ms}^{s'} v_{ms} . \qquad (9)$$

Note $\sigma_{ms}^{s'} < \sigma_{ms}^s$ and $\sigma_{ms}^{s'} = G_{ms}\gamma_b^{'}$ where G_{ms} is the shear modulus of micro-spheres.

Some example facture surfaces for $F_{ms} < F_b$, are found in the literature [6, 7] although Equations (7) - (9) are subject to experimental verification.

3. Constituent materials for manufacturing syntactic foams

3.1. Hollow micro-spheres

Ceramic hollow micro-spheres composed of silica 55-60%, alumina 36-40%, iron oxide 0.4-0.5% and titanium dioxide 1.4-1.6% were supplied by Envirospheres Pty Ltd, Australia. Four different size groups (or commercial grades), SL75, SL150, SL300 and SL500, were employed and sizes were measured using a Malvern 2600C laser particle size analyser - results are listed in **Table 1**. Particle densities and bulk densities of the four hollow micro-sphere groups were also measured using an air comparison pycnometer (Beckman 930) and a measuring cylinder (capacity 250cc) respectively. Three hundred taps were conducted for each bulk density measurement. An average of five measurements was taken for each size group and is listed in **Table 1**.

3.2 Starch as binder

Potato starch (Tung Chun Soy & Canning Company, Hong Kong) was used as binder for hollow ceramic micro-spheres. Particle density of the potato starch was measured using an air comparison pycnometer (Beckman 930) and an average of three measurements was found to be 1.50g/cc. Bulk density was also measured using a measuring cylinder with a tapping device (300 taps were conducted) and an average of five measurements was found to be 0.85g/cc.

4. Manufacturing of syntactic foams for compressive specimens

The basic principles of manufacturing for syntactic foams are given in references [18, 19] as well. Various binder systems by varying starch concentration in water were prepared. Hollow micro-spheres (115 ± 35g) were added to the water-starch mixture placed in a transparent container (120 mm in diameter and 150 mm in height). The volume ratio of bulk micro-spheres to binder was approximately 1 to 3. The resulting mixture was manually shaken up after sealing for at least 90 seconds. The container was left for 5 minutes to allow for phase separation caused by buoyancy of micro-spheres. Top phase consisted of micro-spheres and binder, bottom phase binder and water as sediment, and middle phase water. The top phase was directly transferred using a scoop into a mould. Gelatinization of starch in the mixture was conducted in two different ways of timing. (Gelatinization is a process of converting granule starch into adhesive binder [20].) One was prior to the addition of hollow micro-spheres to water-starch mixture and the other after moulding, which will be referred to as pre- and post-mould gelatinization processes respectively. In the case of pre-mould gelatinization process, the mixture of starch and water was heated until the gelatinization fully occurred. The gelatinization temperature range was measured to be 64-69ºC. Some extra amount of water was added in the starch-water mixture to maintain a constant ratio of starch to water during heating to compensate the loss of water due to evaporation. The mixture was cooled down to room temperature before moulding. Drying after moulding was conducted in an oven for 6 hours at 80°C and further 2 hours after demoulding. In the case of post-mould gelatinization process, filled moulds were placed in an oven at the same temperature (80°C) for 1 hour with aluminium covers on to keep

sufficient moisture/water in the mould for gelatinization, and then for 5 hours without covers for drying in the mould and finally 2 hours further drying at the same temperature after demoulding.

Split cylindrical moulds with a cavity diameter of 16 mm and a height of 24 mm were used for compressive specimens. A final height of 15 mm for each specimen was obtained by grinding with abrasive sheets (P400 and P320). Parallelism of top and bottom specimen surfaces was ensured by measuring five to six different locations of height using a pair of Vernier callipers – variation was within ±1.25% of the average height of specimen.

5. Mechanical tests

Compression tests were conducted on a universal testing machine (Shimadzu 5000) with a Hounsfield compression cage at a crosshead speed of 1.0 mm/min and at an ambient temperature range of 14–18°C. Platens of Hounsfield compression cage were lubricated using engine oil SAE 15-40 to minimise friction between specimen and each platen. Three samples were tested for each starch content in binder. They were compressed until about 20-50% of the initial height of the specimen, which was sufficient to observe the initial breakage and subsequent possible densification. Compressive strength was calculated using the original cross-sectional area. Elastic modulus was determined from the tangent to the initial high linear portion of stress-strain trace.

6. Microscopy

A Philips XL30 and a JEOL JSM-840 Scanning Electron Microscopes were employed for microscopic examinations of specimens coated with gold (20 nanometre thick).

7. Measurements for mass/volume fractions of constituent materials in foams

Mass/volume fractions of constituent materials of the present foams were measured by monitoring various volumes and masses in a confined system during foam manufacturing separately conducted for the measurements. A 400cc binder (water + starch) was placed in a measuring cylinder (50mm in diameter)

and a micro-sphere mass of 25g was added. This was followed by stirring with an aluminium spatula for a couple of minutes. The stirred mixture was left for one hour for phase separation due to buoyancy and then the excess binder (mainly in the form of two phases under the top phase) was drained through a hole at the bottom of the measuring cylinder. The resulting wet foam in the cylinder was dried in an oven at 80°C. The drying was continued until mass of the foam shows no change. It took 12 to 24 hrs depending on micro-sphere size and starch content. At last, dried foam was taken out from the measuring cylinder.

Volume fractions of micro-spheres (v_{ms}), binder (starch) (v_b) and voids (v_v) were measured using [1]:

$$v_v = 1 - (v_{ms} + v_b) = 1 - \rho_{sy}\left(\frac{m_{ms}}{\rho_{ms}} + \frac{m_b}{\rho_b}\right) \tag{10}$$

$$v_{ms} = \rho_{sy}\frac{m_{ms}}{\rho_{ms}} \tag{11}$$

and

$$v_b = \rho_{sy}\frac{m_b}{\rho_b} \tag{12}$$

where ρ is the density, m is the mass fraction, and subscripts (*sy*, *ms* and *b*) denote syntactic foam, micro-sphere and binder (starch), respectively.

8. Results and discussion

The syntactic foams manufactured are of ternary system comprising micro-spheres, starch and voids. Volume fractions (of micro-spheres, starch and voids) for various foams as functions of volume fraction of starch in binder prior to drying are given in **Figure 3**. Given that high starch contents lead to high density and expensive syntactic foams, the current manufacturing method appears useful allowing us to achieve

small volume fractions of starch in syntactic foams. Volume fraction of micro-spheres in foam (**Figure 3(a)**) is seen to be not much affected by starch content in binder (= water + starch before drying) and this trend becomes more prominent for SL500 irrespective of gelatinization timing (e.g. pre- or post-mould gel). The reason for this is that the amount of starch contained in SL500 is relatively small as seen in **Figure 3(b)**. Volume fraction of micro-spheres for SL500 is found to be particularly low compared to others. This appears to be due to an approximately constant high void fraction in SL500 as found in **Figure 3(c)**. Volume fraction of starch in foam (**Figure 3(b)**) is highly proportional to starch content in binder with high correlation coefficients as given in the caption of **Figure 3(b)**. Also it increases as micro-sphere size becomes small and is high for pre-mould gelatinization process.

General features of stress-strain curves resulted from mechanical testing for all micro-sphere size groups were found to be similar to each other. Some typical stress-strain curves represented by SL300 foams are given in **Figure 4** in which various starch contents for both pre- and post-mould gelatinization processes are shown. The maximum stresses (or compressive strengths) generally appear to be followed by the negative slopes and then plateau regions in the case of low starch contents (or low strengths). In the case of high starch contents, however, the low negative slopes tend to be accompanied by some undulation. It was difficult to define a densification stage in a curve. This seems to be due to shear failure mechanism of relatively high aspect ratio of compressive specimens, which will be discussed below because, once shear failure at the maximum stress occurred, sliding of fracture surfaces rather than densification is possible.

It was observed that compressive failure of all the foams is generally either by shear on planes inclined approximately 45^{O} to the loading direction (**Figure 5(a)** and **(c)**) or of 'cup and cone' type with vertical splitting (**Figure 5(b)** and **(d)**). Some SEM images for specimens with various starch contents in foams (prepared with a constant mass ratio of water to starch, 70/1) and various size groups are shown in **Figure 6**. Not many broken micro-spheres are seen on fracture surfaces of low binder contents, indicating that micro-spheres were mainly debonded and hence the failures were governed under the condition of [$F_{ms} > F_b$ and $\sigma_{ms}^{s} > \sigma_{bond}$]. In some other specimens of SL300 containing highest binder contents for both pre- and post-mould gelatinization processes (prepared with a mass ratio of water to starch, 30/1), however, many broken micro-spheres were found on fracture surfaces, indicating the condition of [$F_{ms} > F_b$ and $\sigma_{ms}^{s} > \sigma_{bond}$] was terminated but the condition of [$F_{ms} > F_b$ and $\sigma_{ms}^{s} < \sigma_{bond}$] commenced due to increased

binder content. Note that binder content for all foams in this paper is still sufficiently low to be under the condition of $F_{ms} > F_b$ as seen in **Figure 3(b)**.. On the other hand, it is interesting to find that binder between micro-spheres formed two dimensional webs in some areas, which is obviously dried starch as a result of evaporation of water. It might be possible to trace down contact points of micro-spheres prior to failure using the shape of dried binder. When a micro-sphere is contacted with other two micro-spheres as shown in **Figure 7**, wet binder can be trapped due to capillary action between micro-spheres and dries to form a 2D web. No major difference in microscopic features between pre- and post-mould gelatinization processes was found although pre-mould gelatinization process allows foam to contain more starch than post-mould gelatinization process as discussed in relation with data in **Figure 3**.

Compressive strength (**Figure 8**) and modulus (**Figure 9**) (with specific properties) of all the foams increase with increasing foam density as expected. They also increase as micro-sphere size decreases for a given density although SL500 displays some anomaly compared to others. Gelatinization timing (pre- or post-mould), however, does not seem to affect much compressive strength and modulus for a given volume fraction of starch.

Compressive strength is replotted as a function of volume fraction of dried binder (or starch) and is given in **Figure 10**. In contrast to the previous plot in **Figure 8**, compressive strengths of SL75, SL150 and SL300 are seen to be approximately independent of micro-sphere size group as previously predicted by the rule of mixtures equations. The three size groups have, in fact, similar constant volume fractions of micro-spheres as already shown in **Figure 3**. Therefore, the slopes and positions of line *A*-*B* (in **Figure 1**) for the three size groups are similar and would be approximately in parallel with that of voids–binder axis on the diagram in **Figure 1**. Now, the compressive strength of syntactic foams in region α-β (in **Figure 1**) is directly affected by binder properties irrespective of compressive strength of micro-spheres under the condition of [$F_{ms} > F_b$ and $\sigma_{ms}^{s} > \sigma_{bond}$] and hence Equation (5) or (6) can be employed. (Note that Equation (2) or (3) is not to be used because the condition of [$F_{ms} > F_b$ and $\sigma_{ms} < \sigma_{bond}$] occurred at the end of the range as a result of increase in binder.) Equation (6) is plotted in **Figure 10** and its correlation coefficient was found to be 0.956 with 102MPa (= $C\sigma_{bond}$ in Equation (5)) for the three size groups (SL75, SL150 and SL300) collectively. SL500 micro-spheres were excluded in the collective analysis because they are somewhat different from other size groups of micro-spheres as seen in **Figure 6**. They are

porous, of poor roundness and posses rough surface texture, possibly resulting in different bond strength (σ_{bond}) to other size groups of micro-spheres for a given binder content.

Compressive modulus as a function of binder content is given in **Figure 11**. Similarly to the compressive strength, it is mainly affected by binder content but not much by micro-sphere size. The least square line with a forced intercept at origin is plotted for the three sizes groups (SL75, SL150 and SL300) collectively and its correlation coefficient was found to be 0.937. SL500 was excluded again for the same reason as discussed for the compressive strength. Thus, the compressive modulus of three groups of micro-spheres (SL75, SL150 and SL300) appears to be approximately proportional to the binder content.

9. Conclusions

Ternary system novel syntactic foams composed of hollow ceramic micro-spheres, starch, and voids have been developed. Various parameters such as micro-sphere size, volume fractions of constituents, and gelatinization timing have been investigated for failure behaviour and mechanical properties of the syntactic foams. Compressive failure of all foams was found to be mainly by shear. Some conditions leading to the rule of mixture relationships have been developed for understanding of failure behaviour and compressive/shear strength. The developed rule of mixture relationships for compressive/shear strength were partially verified. It was found that compressive strength and modulus were not much affected by micro-sphere size and gelatinization timing.

Acknowledgements

One of the authors (M. M. Islam) gratefully acknowledges the University of Newcastle Postgraduate Research Scholarship (UNRS) and International Postgraduate Research Scholarship (IPRS). The authors thank Envirospheres Pty Ltd, Australia for supplying ceramic hollow micro-spheres for this study.

References

1. H. S. KIM and P. PLUBRAI, Composites Part A – Applied Science and Manufacturing 35 (2004) p. 1009.

2. M. NARKIS, M. GERCHCOVICH, M. PUTERMAN and S. KENIG, Journal of Cellular Plastics, July/August (1982) p. 230.

3. M. NARKIS, M. PUTERMAN and S.KENIG, Journal of Cellular Plastics, Nov/Dec (1980) p.326.

4. A.R. LUXMOORE and D.R.J. OWEN, in "Mechanics of Cellular Plastics" edited by N. C Hilyard (Applied Science Publishers Ltd, London, 1982) p. 359.

5. E. RIZZI, E. PAPA and A.CORIGLIANO, International Journal of Solids and Structures 37 (2000) 5773.

6. H. S. KIM and H. H. OH, Journal of Applied Polymer Science 76 (2000) 1324.

7. N. GUPTA, KISHORE, E. WOLDESENBET, and S. SANKARAN, Journal of Materials Science 36 (2001) 4485.

8. N. GUPTA, E. WOLDESENBET and KISHORE, Journal of Materials Science 37 (2002) 3199.

9. M. NARKIS, M. PUTERMAN and H. BONEH, Polymer Engineering and Science 22 (1982) 417.

10. E. LAWRENCE, D. WULFSOHN, and R. PYRZ, Polymers and Polymer Composites 9 (2001) 449.

11. E. LAWRENCE and R. PYRZ, Polymers and Polymer Composites 9(2001) 227.

12. H. VERWEIJ, G. DE WITH and D.VEENEMAN, Journal of Materials Science 20 (1985) 1069.

13. M. PUTERMAN and M. NARKIS, Journal of Cellular Plastics, July/August (1980) 223.

14. S. KENIG, I. RAITER and M. NARKIS, Journal of Cellular Plastics, Nov/Dec (1984) 423.

15. C. METEER, Syntactic foam core material for composite structures, International patent classification : B29C, 65/00, B29D 9/00, B32B 3/26, 5/18.

16. H. S. KIM and H. H. OH, in Proceedings of the first ACUN International Composites Meeting on Composites : Innovation and Structural Applications, February 1999, edited by S. BANDYOPADHYAY, N. GOWRIPALAN, S. RIZKALLA, P. DITTA and D. BHATTACHARYYA (University of New South Wales, Sydney, 1999) p. 83.

17. K. TE NIJENHUIS, R. ADDINK, and A. K.VAN DER VEGT, Polymer Bulletin 21 (1989) 467.

18. H. S. KIM, Syntactic foam, International Publication Number: WO 03/074598 A1, International Patent Classification: C08J 9/32, International Patent Application Number: PCT/AU03/00250, International Publication Date: 12 Sept 2003.

19. H. S. KIM, Cenosphere composite and method for preparing same, Australian patent application No: 2004903795. PCT Patent Application No. PCT/AU2005/001009 (Title: Method of forming syntactic foams).

20. W. Banks and C. T. Greenwood, in "Starch and its Components" (Edinburgh University Press, Edinburgh, 1975) p. 259.

Table 1 Particle size ranges and densities of ceramic micro-spheres employed**.**

Hollow micro-spheres	Size range (μm) (approximately 95%)	Particle density (g/cc)	Bulk density (g/cc)
SL75	31 – 83	0.68	0.39
SL150	56 – 183	0.73	0.42
SL300	101 – 332	0.80	0.43
SL500	151 – 600	0.89	0.36

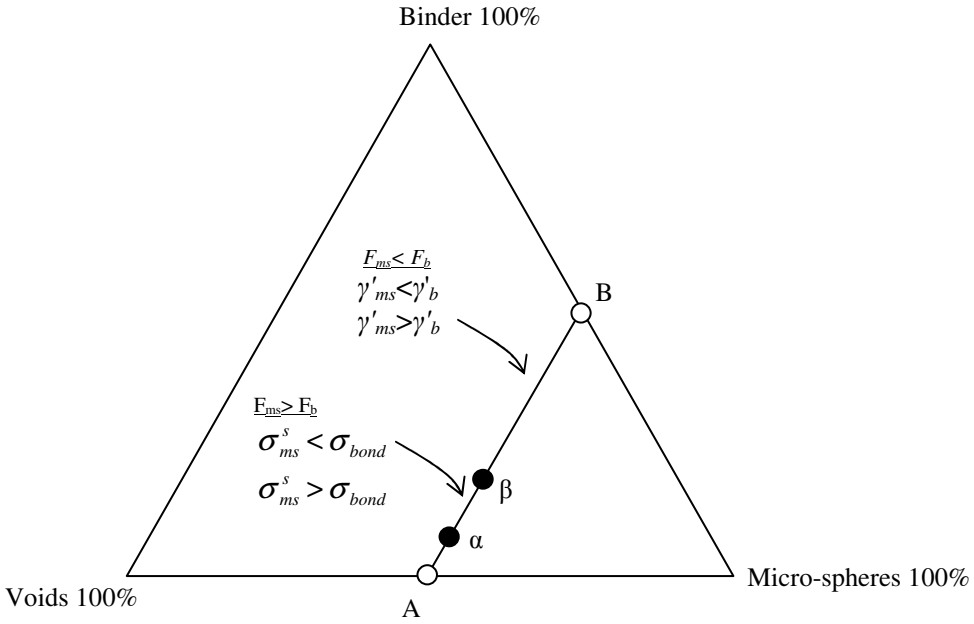

Figure 1 Transitional points and various conditions under compression on the diagram of ternary system.

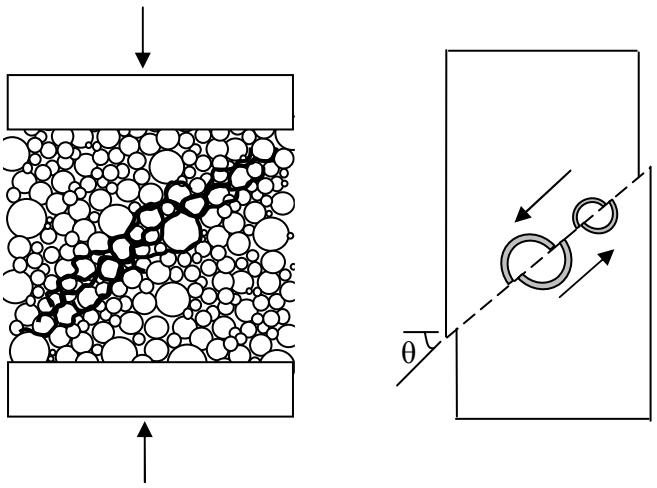

(a) (b)

Figure 2 Shear failure of syntactic foams: (a) debonding area indicated by thick lines; and (b) binder carries load after micro-spheres fail. (Binder and voids are not shown.)

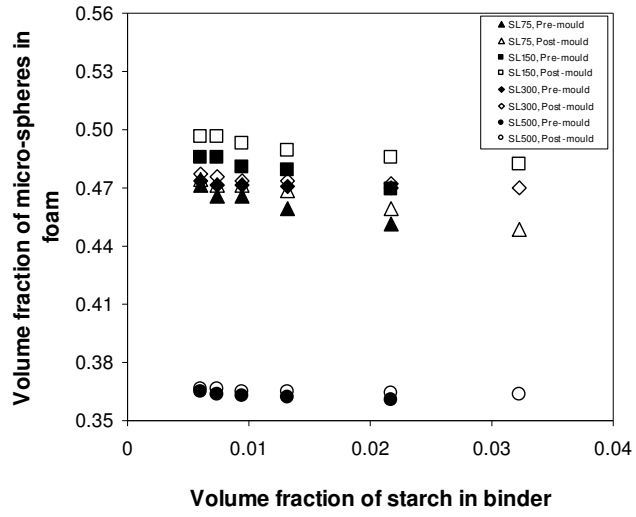

(a)

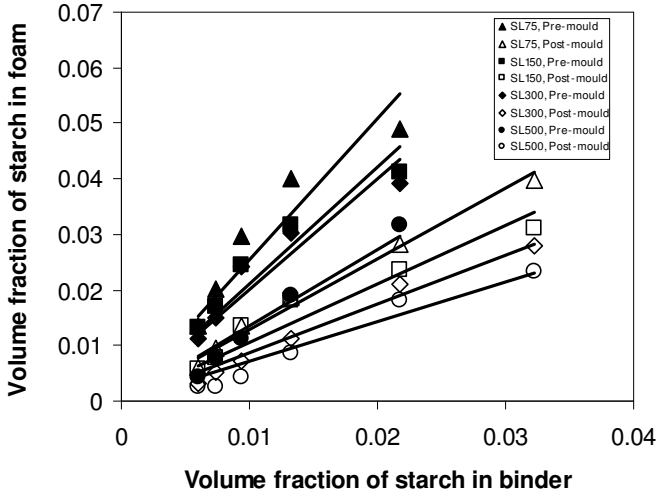

(b)

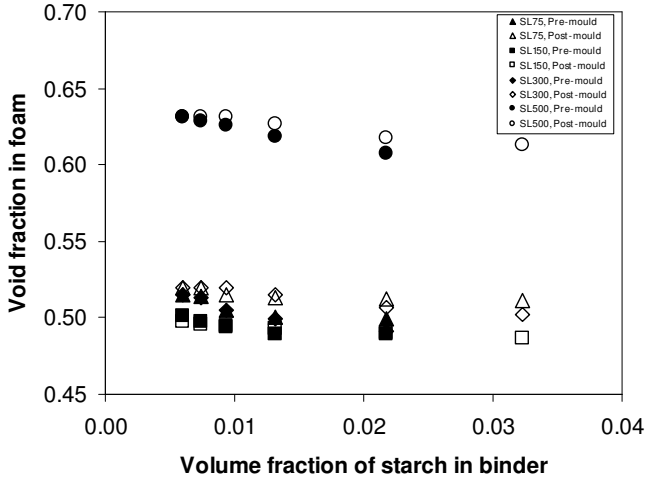

(c)

Figure 3 Various volume fractions for foams manufactured as a function of volume fraction of starch in binder prior to drying: (a) volume fraction of micro-spheres in dried foam; (b) volume fraction of starch in dried foam (correlation coefficients with a forced intercept at zero for SL75 pre = 0.928, SL150 pre = 0.939, SL300 pre = 0.938, SL500 pre = 0.970; SL75 post = 0.993, SL150 post = 0.956, SL300 post = 0.987, SL500 post = 0.969); and (c) void fraction in dried foams.

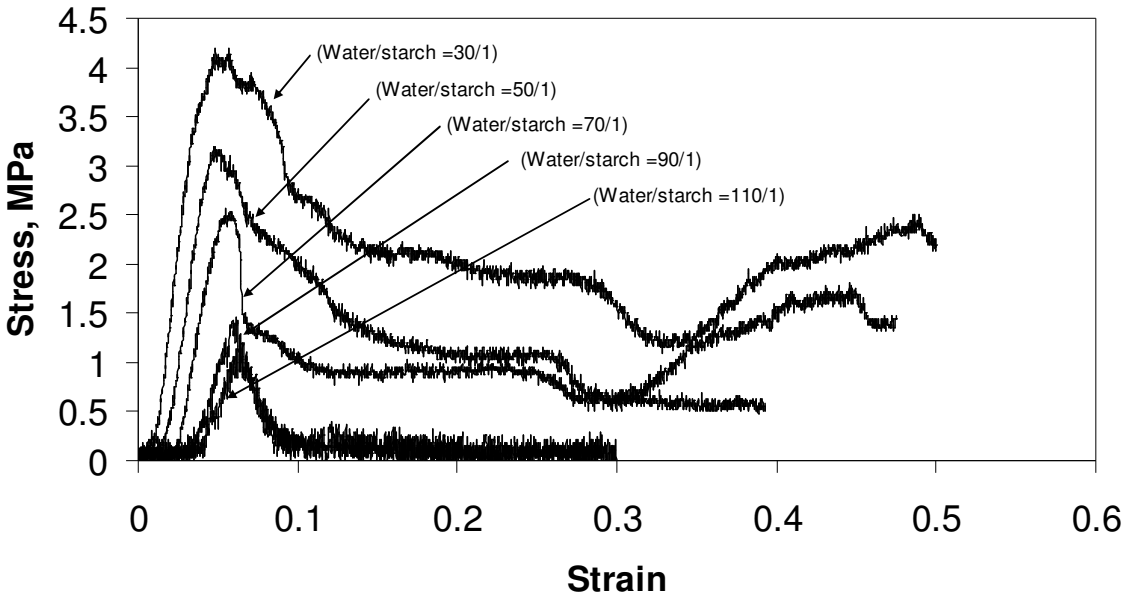

(a)

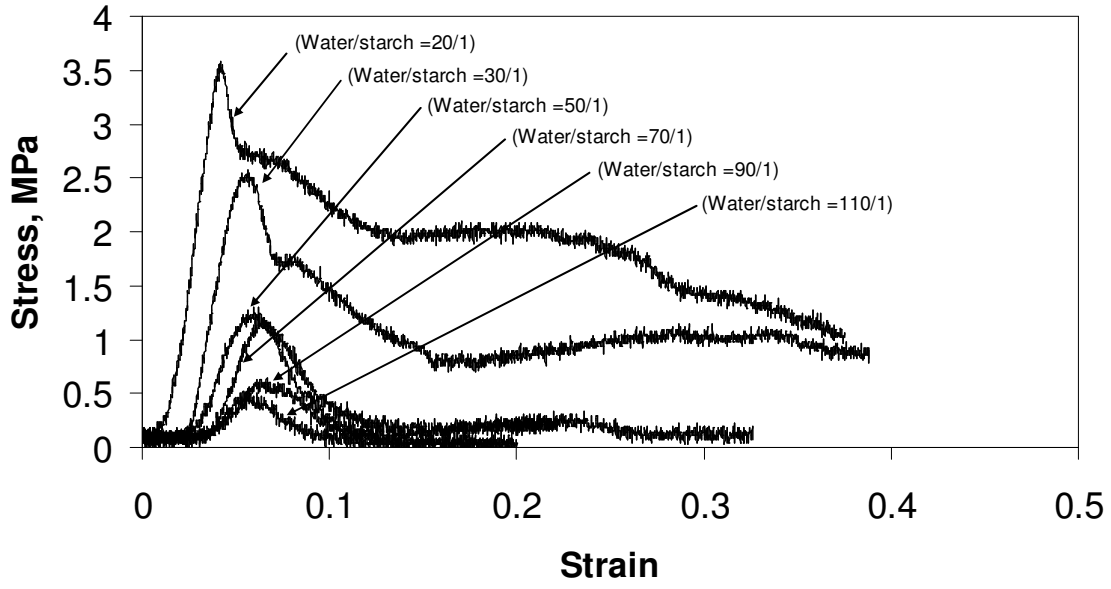

(b)

Figure 4 Typical stress-strain curves (SL300) with mass ratios of water to starch : (a) pre-mould gelatinization process; and (b) post-mould gelatinization process. The mass ratios of water to starch given here correspond with volume fractions of starch in binder in **Figure 3** respectively.

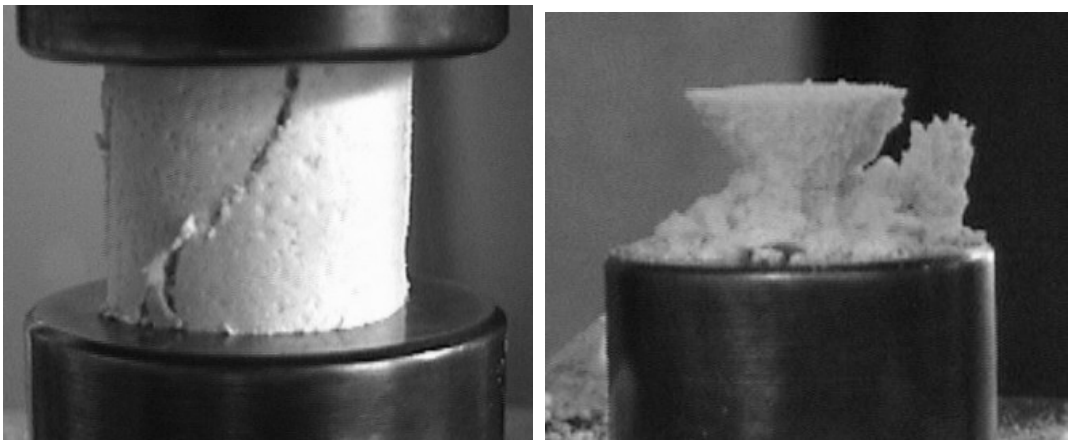

(a) (b)

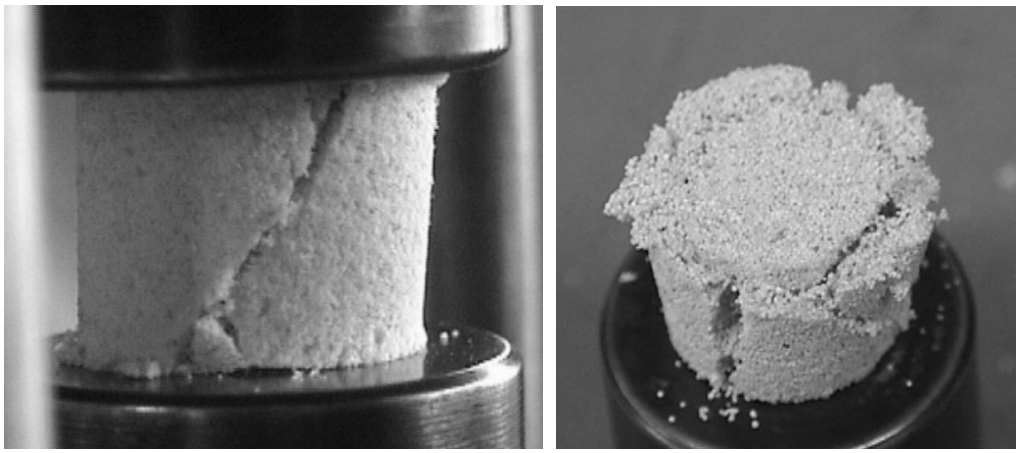

(c) (d)

Figure 5 Some examples of failure mode showing shear on planes inclined about 45^{O} to the loading direction or 'cup and cone' type: (a) SL75, pre-mould gel, mass ratio of water to starch =110/1; (b) SL150, pre-mould gel, mass ratio of water to starch =110/1; (c) SL300, pre-mould gel, mass ratio of water to starch =110/1; and (d) SL500, post-mould gel, mass ratio of water to starch =30/1.

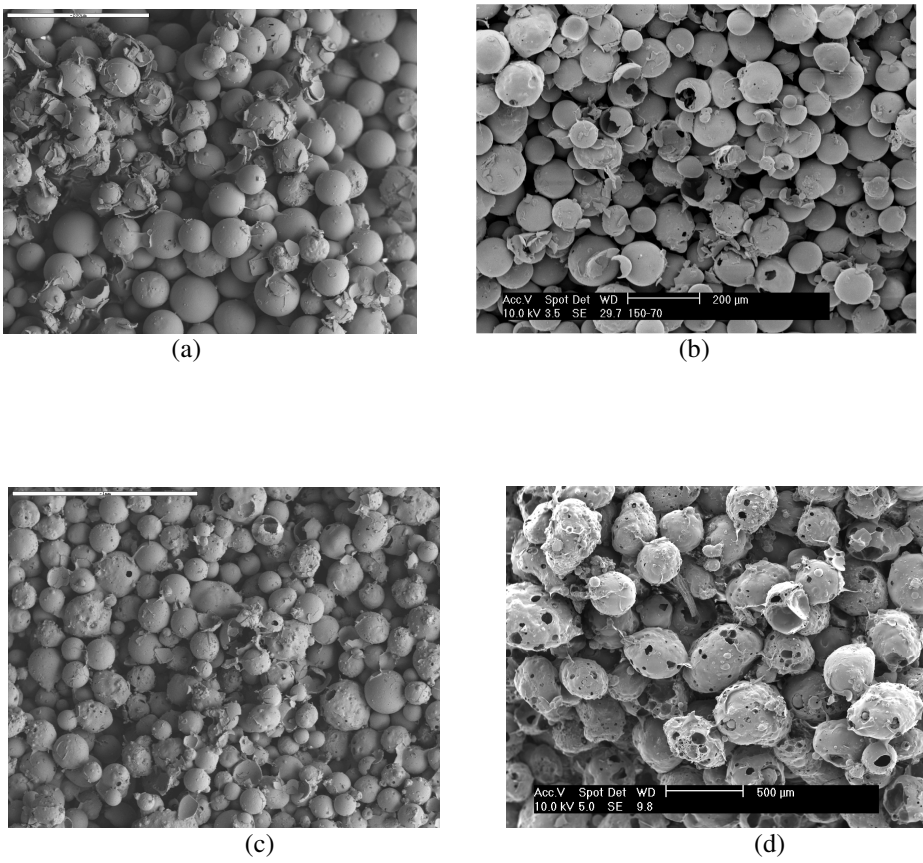

(a) (b)

(c) (d)

Figure 6 SEM images of fracture surfaces of compressive specimens with water/starch=70/1: (a) SL75, v_b = 0.030, pre-mould gel; (b) SL150, v_s = 0.024, pre-mould gel; (c) SL300, v_b = 0.007, post-mould gel; and (d) SL500, v_b = 0.011, pre-mould gel,. The scale bar in '(a)' and '(b)' represents 200µm, in '(c)' 1mm, and in '(d)' 500µm.

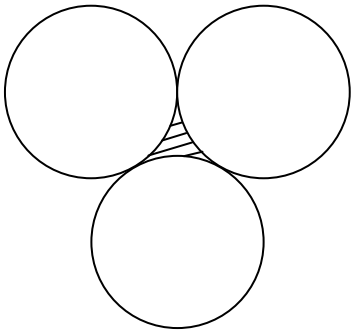

Figure 7 Formation of 2D web on a micro-sphere surface. Hatched area represents binder before drying.

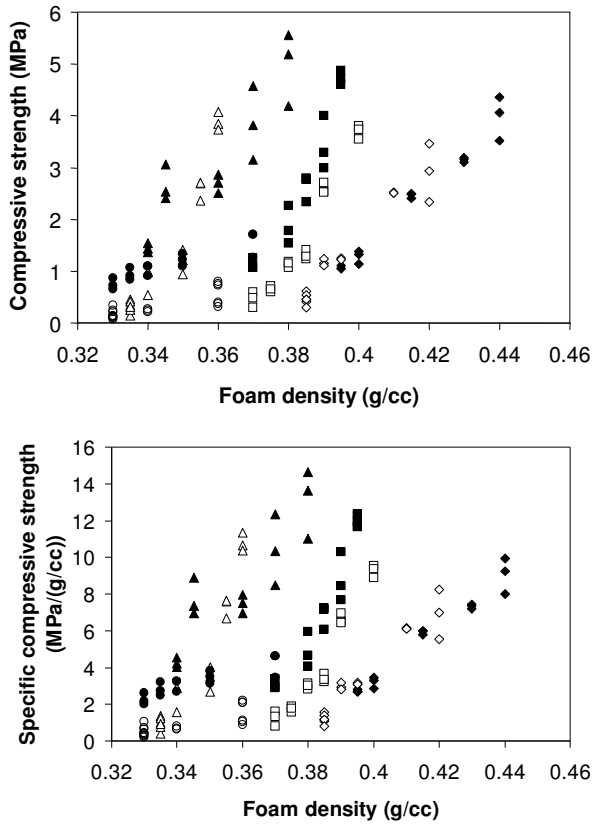

(a) (b)

Figure 8 (a) Compressive strength and (b) specific compressive strength as function of foam density: ▲, SL75 pre-mould gelatinization; Δ, SL75 post-mould gelatinization; ■, SL150 pre-mould gelatinization; □, SL150 post-mould gelatinization; ◆, SL300 pre-mould gelatinization; ◇, SL300 post-mould gelatinization; ●, SL500 pre-mould gelatinization; and ○, SL500 post-mould gelatinization.

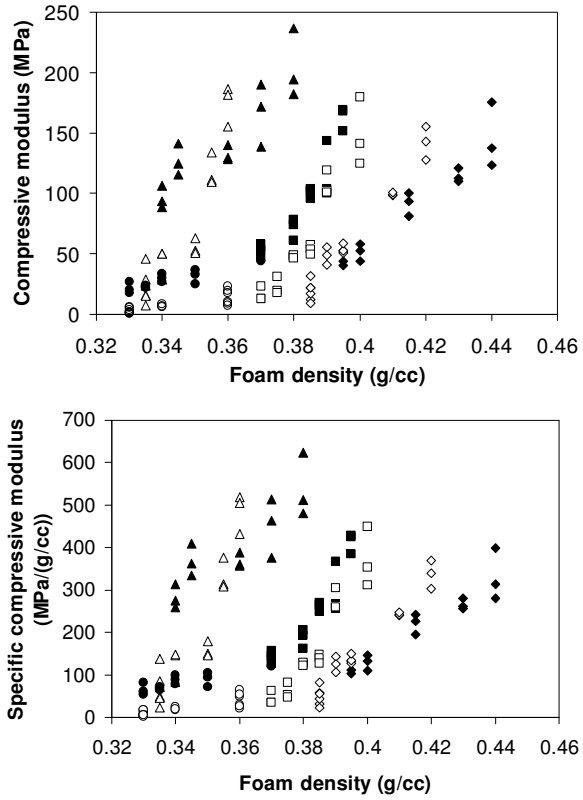

(a) (b)

Figure 9 (a) Compressive modulus and (b) specific compressive modulus as function of foam density: ▲, SL75 pre-mould gelatinization; Δ, SL75 post-mould gelatinization; ■, SL150 pre-mould gelatinization; □, SL150 post-mould gelatinization; ◆, SL300 pre-mould gelatinization; ◇, SL300 post-mould gelatinization; ●, SL500 pre-mould gelatinization; and ○, SL500 post-mould gelatinization.

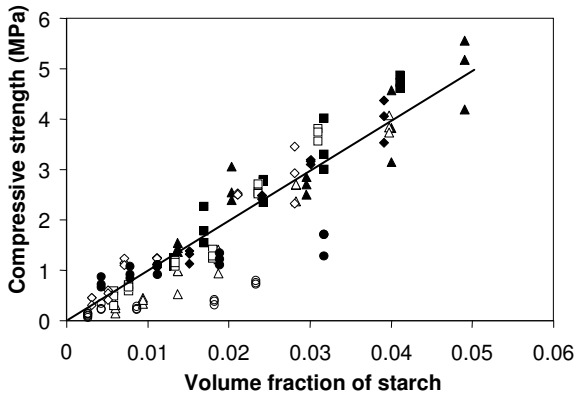

Figure 10 Compressive strength as function of volume fraction of starch in foam: ▲, SL75 pre-mould gelatinization; Δ, SL75 post-mould gelatinization; ■, SL150 pre-mould gelatinization; □, SL150 post-mould gelatinization; ◆, SL300 pre-mould gelatinization; ◇, SL300 post-mould gelatinization; ●, SL500 pre-mould gelatinization; and ○, SL500 post-mould gelatinization. The least square line is for SL75, SL150 and SL300 collectively.

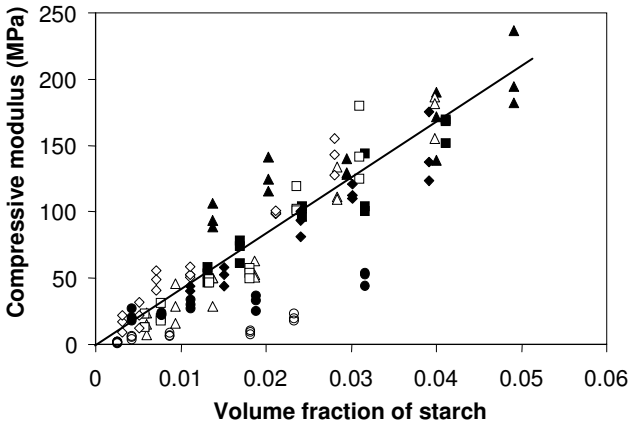

Figure 11 Compressive modulus as a function of volume fraction of starch in foam: ▲, SL75 pre-mould gelatinization; Δ, SL75 post-mould gelatinization; ■, SL150 pre-mould gelatinization; □, SL150 post-mould gelatinization; ◆, SL300 pre-mould gelatinization; ◇, SL300 post-mould gelatinization; ●, SL500 pre-mould gelatinization; and ○, SL500 post-mould gelatinization. The least square line is for SL75, SL150 and SL300 collectively.